THE JOURNAL OF BIOLOGICAL CHEMISTRY VOL. 288, NO. 20, pp. 13974–13987, May 17, 2013

Competition between Core-2 GlcNAc-transferase and ST6GalNAc-transferase Regulates the Synthesis of the Leukocyte Selectin Ligand on Human P-selectin Glycoprotein Ligand-1*[S]

Received for publication, February 21, 2013, and in revised form, March 26, 2013 Published, JBC Papers in Press, April 2, 2013, DOI 10.1074/jbc.M113.463653

Chi Y. Lo[‡], Aristotelis Antonopoulos[§], Rohitesh Gupta[‡], Jun Qu[¶‖], Anne Dell[§], Stuart M. Haslam[§], and Sriram Neelamegham[‡‖1]

From the [‡]Department of Chemical and Biological Engineering, [¶]Pharmaceutical Sciences, and [‖]The New York State Center for Excellence in Bioinformatics and Life Sciences, The State University of New York, Buffalo, New York 14260 and the [§]Department of Life Sciences, Faculty of Natural Sciences, Imperial College London, London, SW7 2AZ, United Kingdom

Background: Carbohydrate epitopes at the N terminus of PSGL-1 (P-selectin glycoprotein ligand-1) facilitate leukocyte binding to selectins.
Results: *O*-linked glycan microheterogeneity analysis at the PSGL-1 N terminus demonstrates the presence of both the core-2 sialyl Lewis-X (sLe^X) and di-sialylated T-antigen.
Conclusion: Overexpression of ST6GalNAc-transferases reduced both sLe^X expression and selectin-mediated leukocyte adhesion.
Significance: ST6GalNAc2 is a novel enzyme that regulates leukocyte adhesion under fluid shear.

The binding of selectins to carbohydrate ligands expressed on leukocytes regulates immunity and inflammation. Among the human selectin ligands, the *O*-linked glycans at the N-terminus of the leukocyte cell-surface molecule P-selectin glycoprotein ligand-1 (PSGL-1, CD162) are important because they bind all selectins (L-, E-, and P-selectin) with high affinity under hydrodynamic shear conditions. Analysis of glycan microheterogeneity at this site is complicated by the presence of 72 additional potential *O*-linked glycosylation sites on this mucinous protein. To overcome this limitation, truncated forms of PSGL-1, called "PSGL-1 peptide probes," were developed. Ultra-high sensitivity mass spectrometry analysis of glycans released from such probes along with glycoproteomic analysis demonstrate the presence of both the sialyl Lewis-X (sLe^X) and the di-sialylated T-antigen (NeuAcα2,3Galβ1,3(NeuAcα2,6)GalNAc) at the PSGL-1 N-terminus. Overexpression of glycoprotein-specific ST6GalNAc-transferases (ST6GalNAc1, -2, or -4) in human promyelocytic HL-60 cells altered glycan structures and cell adhesion properties. In particular, ST6GalNAc2 overexpression abrogated cell surface HECA-452/CLA expression, reduced the number of rolling leukocytes on P- and L-selectin-bearing substrates by ~85%, and increased median rolling velocity of remaining cells by 80–150%. Cell rolling on E-selectin was unaltered although the number of adherent cells was reduced by 60%. ST6GalNAc2 partially co-localizes in the Golgi with the core-2 β(1,6)GlcNAc-transferase C2GnT-1. Overall, the data describe the glycan microheterogeneity at the PSGL-1 N-terminus. They suggest that a competition between ST6GalNAc2 and C2GnT-1 for the core-1/Galβ1,3GalNAc glycan may regulate leukocyte adhesion under fluid shear.

P-selectin glycoprotein ligand-1 (PSGL-1,[2] CD162) is a leukocyte cell surface molecule that binds all three members of the selectin family (L-, E- and P-selectin) with high affinity under fluid shear conditions (1–3). By engaging the selectins in blood circulation, PSGL-1 facilitates leukocyte trafficking to sites of inflammation. In addition to this, recent studies suggest that PSGL-1 also binds chemokines, like CCL19 and CCL21 (4). This PSGL-1-chemokine binding interaction partially regulates resting T-cell homing to secondary lymphoid organs (5).

From the structural standpoint, PSGL-1 is a type I transmembrane homodimeric mucinous glycoprotein with a monomer molecular mass of ~120 kDa (1) (Fig. 1*A*). The first 41 amino acids of PSGL-1 include an 18-amino acid signal peptide and a cleavable propeptide. The mature protein, which starts at residue 42, includes an N-terminal peptide segment that is followed by an *O*-glycan-rich decamer repeat section (6). Polymorphisms in PSGL-1 result in humans containing between 14 and 16 decamer repeat units (7), with the human promyelocytic leukemia HL-60 cell line having 15 decamer repeats that span residues 118–279 (8). The extracellular section of PSGL-1 is decorated by 73 potential sites for *O*-linked glycosylation and three *N*-linked glycans. Among these, a sialofucosylated *O*-glycan at Thr-57 is essential for P- and L-selectin binding,

* This work was supported, in whole or in part, by National Institutes of Health Grants HL63014 and HL103411 (to S. N.). This work was also supported by an American Heart pre-doctoral fellowship (to C. Y. L.) and Biotechnology and Biological Sciences Research Council Grants B19088 and BBF0083091 (to A. D. and S. M. H.).
[S] This article contains supplemental Methods, Tables S1–S3, Figs. S1–S5, and Movies A and B.
[1] To whom correspondence should be addressed: 906 Furnas Hall, State University of New York, Buffalo, NY 14260. Tel.: 716-645-1200; Fax: 716-645-3822; E-mail: neel@buffalo.edu.

[2] The abbreviations used are: PSGL-1, P-selectin glycoprotein ligand-1; EF1α, elongation factor-1 α; DBCO, dibenzylcyclooctyne; EK, enterokinase; Ab, antibody.

whereas additional sites may also recognize E-selectin (9, 10). Accumulating evidence suggests that this N-terminal PSGL-1 site contains a glycan with the core-2 motif (Galβ1,3(GlcNAcβ1,6)GalNAc) linked to a terminal sialyl Lewis-X (NeuAcα2,3Galβ1,4(Fucα1,3)GlcNAc-, sLe^X) or related epitope (11, 12). Sulfation of tyrosine residues in the proximity of this glycan enables P- and L-selectin binding under hydrodynamic shear (13, 14). After the mucinous decamer repeat region of PSGL-1 is a 20-amino acid transmembrane and 70-amino acid cytoplasmic section.

Previous studies identified the *O*-glycans of PSGL-1 by purifying this protein from HL-60 cells and characterizing all the glycans released from it by β-elimination (15, 16). Glycans released in these previous studies were separated by conventional lectin and column (ion exchange and size exclusion) chromatography along with various enzymatic digestions to decipher the *O*-glycan structures. These studies showed that 14–37% of the PSGL-1 *O*-glycans contain the core-1 motif (Galβ1,3GalNAc), whereas the remaining contain the trisaccharide core-2 motif (Table 1). Furthermore, although 4.7–14% of the *O*-glycans express the terminal sLe^X structure, only ~2% of the glycans bear sLe^X on non-extended mono-lactosamine core-2 chains. Whereas these studies provide valuable information regarding the overall distribution of *O*-glycans on PSGL-1, the specific structures located at Thr-57 and the glycan microheterogeneity at this site remain unknown.

Determination of the microheterogeneity of a single glycosylation site in a mucinous protein is complicated due to the high density of *O*-glycans and the abundance of proline residues that complicate glycoproteomic analysis. To overcome these limitations, a family of PSGL-1 peptide probes was developed. In these molecules the N-terminal section of PSGL-1, which contains the major selectin binding epitope, was retained, whereas the mucin-rich decamer repeat region was replaced with a human IgG1 Fc, which lacks *O*-glycans. These probes were expressed in HL-60s, as PSGL-1 from HL-60 and primary human neutrophils are functionally similar (1, 17). *O*- and *N*-glycans released from these peptide probes were characterized using mass spectrometry (MS), and glycoproteomic analysis was used to verify the site specificity of the identified glycans. The study demonstrates that the *O*-glycan microheterogeneity at the N terminus is different from the overall PSGL-1 *O*-glycan distribution reported previously (15, 16). In particular, in addition to the core-2 sLe^X structure, a novel disialylated T-antigen glycan exists at the PSGL-1 N terminus. Furthermore, a competition between the α(2,6)sialyltransferase ST6GalNAc2 and core-2 *N*-acetylglucosaminyltransferase C2GnT-1 regulates the relative expression of the di-sialylated T-antigen and the sLe^X epitope at Thr-57. This regulation may impact both selectin-ligand biosynthesis, which controls leukocyte adhesion rates under fluid flow, and chemokine binding, which regulates T-cell homing.

EXPERIMENTAL PROCEDURES

Cell Culture—CHO-S cells (Invitrogen), CHO-S stably expressing P-selectin (CHO-P), HEK293T (ATCC, Manassas, VA), and variants of HEK293T were cultured in Dulbecco's modified Eagle's medium containing 10% FBS. HL-60 cells and various cell lines derived from this were maintained in Iscove's modified Dulbecco's medium with 10% FBS. Mouse fibroblast L cells stably expressing human E-selectin (L-E cells) were cultured in RPMI 1640 with 10% FBS, 0.25 mg/ml xanthine, hypoxanthine-thymidine supplement, and 5 μg/ml mycophenolic acid.

Glycosyltransferase and PSGL-1 Protein Probe Expression—Molecular biology procedures outlined in supplemental Methods were applied to construct lentiviral plasmids that encode for glycosyltransferases and PSGL-1 variants. (i) Three plasmids aimed to optimize gene expression in HL-60 leukocytes include either the cytomegalovirus (CMV), elongation factor-1 α (EF1α), or phosphoglycerate kinase (PGK) promoter driving the expression of a fluorescent DsRED reporter (red fluorescent protein variant). (ii) A plasmid encoding FUT7-DsRed fusion protein was used to generate a HEK293T variant that stably overexpresses the human α(1,3) fucosyltransferase FUT7, called $FUT7^+$HEK cells. (iii) Three plasmids encoding ST6GalNAc1, -2, or -4 followed by an internal ribosome entry site and DsRED reporter were used to express glycosyltransferases in HL-60 cells. Transduction of HL-60 with these constructs resulted in $ST6GalNAc1^+$, $ST6GalNAc2^+$, and $ST6GalNAc4^+$ HL-60 cell lines, respectively. (iv) For glycosyltransferase co-localization studies in HEK293T cells, the vectors contained cDNA that encoded either ST6GalNAc2-DsRED or C2GnT-1-EGFP fusion proteins. (v) Cell-surface protein expression vectors encoded full-length PSGL-1, 19FcTM, or 76FcTM. In the last two molecules, the first 19 or 76 amino acids of mature PSGL-1 were followed by human Fc, PSGL-1 transmembrane and cytoplasmic domains, and finally a poly-His tag. (vi) Soluble, secreted forms of PSGL-1 that were expressed include 19Fc, 19Fc[T57A], and 19Fc[P62A]. Among these, 19Fc encodes for the first 19 amino acids of mature PSGL-1 followed by an enterokinase cleavage site, the human Fc, and poly-His tag (supplemental Fig. S1). 19Fc[T57A] and 19Fc[P62A] are identical to 19Fc, only they either lack the critical selectin binding *O*-glycan at Thr-57 or include a new trypsin cleavage site at the carboxyl side of Arg-61. These constructs (19Fc, 19Fc[T57A], and 19Fc[P62A]) were expressed in wild-type HL-60. 19Fc was also expressed in $ST6GalNAc2^+$ HL-60s, and the product formed is called $19Fc[ST6GalNAc2^+]$. Except for the promoter optimization study, the CMV promoter drove expression of all constructs in HEK293T cells, whereas the EF1α promoter was used for constructs expressed in HL-60 cells.

Lentiviruses were created for each of the above constructs (supplemental Methods). These were introduced into HEK293T and HL-60 to achieve stable gene expression (18, 19).

19Fc Purification and Characterization—HEK293T and HL-60 cells that express soluble 19Fc and its variants were scaled up to 20–25 T-150 flasks. After scale-up, the cells were washed extensively with phosphate-buffered saline (PBS), and culture media was changed to serum-free Pro293a (Lonza, Walkersville, MD). Supplemental Table S1 compares HL-60 cell growth and 19Fc production in different serum-free media. Cell culture supernatant, collected after 3 days, was centrifuged and passed through a 0.2 μm filter. His-tagged protein was then captured onto a HisTrap HP column using an AKTA FPLC system (GE Healthcare), the column was washed with sodium

phosphate buffer (20 mM sodium phosphate, 500 mM NaCl, pH 7.4) containing 25–100 mM imidazole, and the bound protein was eluted using sodium phosphate buffer containing 200 mM imidazole. The collected 19Fc fractions were resolved using 4–20% gradient SDS-PAGE (Thermo-Pierce, Rockford, IL). Proteins were detected either using silver stain or by transferring them to nitrocellulose membranes for Western blotting with either anti-PSGL-1 mAb KPL-1 (BD Pharmingen) or anti-human IgG Ab (Jackson ImmunoResearch, West Grove, PA). 19Fc obtained using the above protocol was at 0.5–3.3 mg/ml.

Metabolic Incorporation of Acetylated N-Azidoacetylmannosamine into 19Fc—HL-60 stably expressing soluble 19Fc were cultured in media containing 50 μM acetylated *N*-azidoacetylmannosamine (Invitrogen) for 3 days. The supernatant was collected, and 19Fc was purified using MagneHis nickel particles (Promega, Madison, WI). After two washes with sodium phosphate buffer (20 mM sodium phosphate, 500 mM NaCl, pH 7.4) containing 10 mM imidazole and an additional wash in the same buffer containing 25 mM imidazole, 19Fc was eluted using buffer containing 500 mM imidazole. The eluted sample was reacted with 200 μM dibenzylcyclooctyne (DBCO)-PEG4-biotin conjugate (Click Chemistry Tools, Scottsdale, AZ) for 3 h at room temperature. After this, 19Fc was separated from unreacted DBCO-PEG4-biotin using a Zeba spin column (Thermo-Pierce). Half of the protein was digested with 0.03 μg/ml enterokinase (EK) (New England Biolabs, Ipswich, MA) overnight at room temperature in 20 mM Tris-HCl, 200 mM NaCl, and 2 mM $CaCl_2$, pH 7.2. Next, both the samples with or without EK were buffer-exchanged to 20 mM ammonium bicarbonate, pH 8. Protein was denatured by heating to 95 °C for 10 min in the presence of 0.02% SDS and 10 mM β-mercaptoethanol. After cooling, 0.42% Nonidet P-40 was added. Both samples were then split into two, and 25 units/μl peptide *N*-glycosidase F (New England Biolabs) was added to half for 2.5 h at 37 °C. Proteins were then resolved using 4–20% gradient SDS-PAGE under standard reducing conditions. Western blot analysis was performed using either anti-PSGL-1 mAb KPL-1, anti-human IgG Ab, or anti-biotin Ab.

Glycomics—19Fc and 19Fc[ST6GalNAc2$^+$] from HL-60 were treated as described previously (20). Briefly all samples were subjected to reduction in 4 M guanidine HCl (Thermo-Pierce) containing 2 mg/ml dithiothreitol, carboxymethylation, and trypsin digestion, and the digested glycoproteins were purified by C_{18}-Sep-Pak (Waters Corp., Hertfordshire, UK). *N*-Linked glycans were released by peptide *N*-glycosidase F (Roche Applied Science) digestion, whereas *O*-linked glycans were released by reductive elimination. *N*- and *O*-glycans were then permethylated using the NaOH procedure, and finally, the permethylated *N*- and *O*-glycans were purified by C_{18}-Sep-Pak.

All permethylated samples were dissolved in 10 μl of methanol, and 1 μl of dissolved sample was premixed with 1 μl of matrix (for MS, 20 mg/ml 2,5-dihydroxybenzoic acid in 70% (v/v) aqueous methanol; for MS/MS, 20 mg/ml 3,4-diaminobenzophenone in 75% (v/v) aqueous acetonitrile). The mixture was then spotted onto a target plate (2 × 0.5 μl) and dried under a vacuum. MS data were acquired using a Voyager-DE STR MALDI-TOF (Applied Biosystems, Darmstadt, Germany). MS/MS data were acquired using a 4800 MALDI-TOF/TOF (Applied Biosystems) mass spectrometer. The collision energy was set to 1 kV, and argon was used as the collision gas. The 4700 calibration standard kit, Calmix (Applied Biosystems), was used as the external calibrant for MS mode of both instruments, and [Glu1] fibrinopeptide B human (Sigma) was used as an external calibrant for the MS/MS mode of the MALDI-TOF/TOF instrument.

The MS and MS/MS data were processed using Data Explorer 4.9 Software (Applied Biosystems). The spectra were subjected to manual assignment and annotation with the aid of GlycoWorkBench (21). The proposed assignments for the selected peaks were based on ^{12}C isotopic composition together with knowledge of the biosynthetic pathways. The proposed structures were then confirmed by data obtained from MS/MS experiments.

Glycoproteomics—19Fc and 19Fc[P62A] from HL-60 were denatured and reduced using 6 M guanidine hydrochloride and 5 mM tris(2-carboxyethyl)phosphine at 95 °C for 10 min. After cooling to room temperature, 50 mM fresh iodoacetamide was added for 30 min in the dark. Buffer was then exchanged to 0.1 M sodium phosphate, pH 8.0, and 1:20 (w/w) enzyme-to-protein ratio of sequencing grade endoproteinase Glu-C (Thermo-Pierce) or trypsin (Thermo-Pierce) was added for 18 h at 37 °C. 6 μg of digested samples prepared in this manner were analyzed using an LTQ-OrbitrapXL mass spectrometer (Thermo Scientific, San Jose, CA). For mobile phase A and B, 0.1% formic acid in 2% acetonitrile and 0.1% formic acid in 88% acetonitrile were used, respectively. Samples were loaded onto a large-ID trap (300-μm inner diameter × 1 cm, packed with Zorbax 3 μm C_{18} material) with 1% B at 10 μl/min. The trap was washed for 3 min before the samples were back-flushed onto the nano-LC column (75 μm inner diameter × 75 cm, packed with Pepmap 3-μm C_{18} material). A 2-h elution with a flow rate of 250 nl/min at 52 °C was employed for separation: 3–8% B over 5 min; 8–24% B over 85 min; 24–38% B over 15 min; 38–63% B over 10 min; 63–97% B in 5 min. Initial MS^1 analysis (m/z 300–2000) was performed at a mass resolution of 100,000 followed by data-dependent MS^2 fragmentation of the seven most abundant precursors in the MS^1 spectra by collision-induced dissociation at a resolution of 30,000.

A suite of MATLAB (MathWorks, Natick, MA) programs called GlycoProteomics Analyzer[3] was written to analyze MS experiments. To this end, .dta files corresponding to the MS runs were generated using BioWorks SEQUEST (Thermo Scientific). In GlycoProteomics Analyzer, a library of potential glycopeptides formed upon digestion of 19Fc and 19Fc[P62A] using either Glu-C or trypsin was generated using knowledge of potential glycans identified in the glycomics analysis (previous section). Variable methionine oxidation and fixed cysteine carbamidomethyl modification was allowed. If an experimentally measured MS^1 precursor ion mass matched the theoretical mass within 20 ppm, the theoretical "candidate glycopeptides" identified was fragmented *in silico* to generate a theoretical MS^2 collision-induced dissociation spectra. Cross-correlation analysis (*Xcorr*) and probability-based (p value) scoring based on the binomial distribution were used to compare the theoretical

[3] S. Neelamegham and C. Y. Lo, unpublished data.

spectra with the experimental MS^2 fragmentation spectra (22, 23). Top hits identified in this manner were annotated.

RNA Isolation and RT-PCR—All human subject protocols were approved by the University at Buffalo Health Science Institutional Review Board. Human neutrophils were isolated from blood obtained from healthy human volunteers by venipuncture into 10 units/ml heparin (17). RNA isolation and RT-PCR were performed as described previously (17). Primers used are listed in supplemental Table S2. Amplified products were run on a 2% agarose gel to confirm molecular weight. The products were also verified by DNA sequencing.

Glycosyltransferase Assay—α(2,3)-sialylated fetuin was used as the substrate to measure ST6GalNAc-transferase activity. This was prepared by covalently coupling fetuin (Sigma) onto 6-μm carboxylate microspheres (PolySciences, Warrington, PA) using carbodiimide chemistry (17). $0.5 \times 10^6/\mu$l fetuin beads were then de-sialylated using 0.2 units/ml α(2,3/6/8/9) *Arthrobacter ureafaciens* neuraminidase (EMD Biosciences, San Diego, CA) for 1 h at 37 °C. The beads were then washed, resuspended at $\sim 0.5 \times 10^6/\mu$l, and then incubated with 0.25 milliunits of rat α(2,3)(*O*) and α(2,3)(*N*) sialyltransferase (EMD Biosciences) and 1.6 mM CMP-NeuAc (Sigma) for 16 h at 37 °C. The final beads are called "α(2,3)sialylated fetuin beads."

For the enzymatic reaction, 0.5×10^6 α(2,3)-sialylated fetuin beads/μl suspended in 100 mM sodium cacodylate, pH 6.0, were incubated with 6.826 μM CMP-[^{14}C]NeuAc (0.0024 μCi, American Radiolabeled Chemicals, St. Louis, MO) and 3 mg/ml HL-60 cell lysate at 37 °C for 6 h (24). After the reaction, the beads were washed extensively using PBS containing 1% BSA. A fraction of this product was left untreated, whereas the remaining material was incubated with either 0.5 units/ml α(2,3/6/8/9) neuraminidase *A. ureafaciens* or 0.5 units/ml α(2,3) neuraminidase *Macrobdella decora* for 1 h at room temperature. After two additional washes, any unreacted CMP-[^{14}C]NeuAc was separated from the beads using silica gel 60 RP-TLC plates (EMD Biosciences) using water containing 0.2% acetic acid as the mobile phase. The TLC plates were then dried, imaged using phosphorimaging, and analyzed using NIH-ImageJ (Bethesda, MD). The amount of ST6GalNAc-transferase activity was quantified in units of dpm product formed per mg of cell lysate.

Confocal Microscopy—HEK293T cells were plated onto glass coverslips coated overnight with 0.1 mg/ml poly-D-lysine (Sigma). Cells were cultured on this substrate for 2 days and fixed with 4% paraformaldehyde containing 2 mM $CaCl_2$ at 37 °C for 15 min, and then these slides were blocked and permeabilized with PBS containing 0.2% Triton X, 1% BSA, and 5% normal goat serum for 1.5 h at room temperature. Fixed slides were then stained with 0.11 μg/ml DAPI for 15 min at room temperature, mounted on microscope slides using ProLong Gold (Invitrogen), and imaged using a Zeiss LSM 710 Axio-Observer confocal microscope (Jena, Germany) equipped with a Plan-Apochromat 63×/1.40 Oil DIC M27 objective. Colocalization overlap coefficient was calculated using the ImageJ plugin JACoP, "Just Another Colocalization Plugin" (25).

Flow Cytometry—Adherent cells were released from tissue culture plastic using PBS containing 5 mM EDTA, washed, and resuspended in HEPES buffer (30 mM HEPES, 110 mM NaCl, 10 mM KCl, 1 mM $MgCl_2$, pH 7.2). Cells cultured in suspension were washed and resuspended in the same buffer. All antibodies used including isotype control reagents were from BD Biosciences unless otherwise mentioned. Mouse monoclonal antibodies used include anti-PSGL-1/CD162 mAb KPL-1, anti-Lewis-X/CD15 mAb HI98, anti-sialyl Lewis-X (sLe^X)/CD15s mAb CSLEX-1, anti-CD65s mAb VIM-2 (AbD Serotec, Raleigh, NC), anti-cutaneous lymphocyte associated antigen/CLA mAb HECA-452, and mAb CHO-131 (R&D Systems, Minneapolis, MN). Among these, HECA-452 primarily recognizes the sLe^X/CD15s glycan on HL-60 cells and CHO-131 binds *O*-linked core-2 sialofucosylated sLe^X (26). A fusion protein containing the human P-selectin lectin and epidermal growth factor domains fused to human IgG was available from a previous study (27). Flow cytometry experiments utilized a FACSCalibur flow cytometer (BD Biosciences), and they followed standard methodologies (18).

Cell Adhesion in Suspension—Viscometry experiments measured the binding of P-selectin bearing activated platelets to beads bearing PSGL-1 variants or HL60 cells (28). Here, anti-human IgG Ab (Jackson ImmunoResearch) was covalently coupled to 6 μm carboxylate microspheres using carbodiimide chemistry (17). 0.5 μg/ml 19Fc or its variants were incubated with these beads to generate "19Fc beads," "19Fc[ST6GalNAc2$^+$] beads," "19Fc[P62A] beads," or "19Fc[T57A] beads." HL-60 were labeled by incubation with 2.7 μg/ml LDS751 (Invitrogen) for 5 min at 37 °C. Platelet-rich plasma was obtained by centrifugation of freshly drawn human blood in 1:9 4% (w/v) sodium citrate (Sigma) at 150 × *g* for 12 min. Platelets were labeled with 0.5 nM BCECF (2′-7′-bis(carboxyethyl)-5(6)-carboxyfluorescein). 2×10^6/ml labeled platelets stimulated using 18 μM TRAP-6 (thrombin receptor agonist peptide) for 5 min at room temperature were shear-mixed with either 2×10^6/ml HL-60 cells or beads in a cone-plate viscometer (VT550, Thermo-Haake, Newington, NH) in HEPES buffer containing 1.5 mM $CaCl_2$ and 0.1% v/v HSA (human serum albumin). Applied shear rate varied from 350/s to 4650/s. A 10 μl sample withdrawn at the indicated times was diluted in 150 μl of HEPES buffer and read immediately using a FACSCalibur flow cytometer. HL-60-platelet and bead-platelet adhesion quantify the percentage of HL-60/beads that are bound to platelets.

Cell Adhesion to Selectin-bearing Substrates under Fluid Shear—HL-60 cells were perfused over substrates bearing either recombinant L-selectin, P-selectin bearing CHO-P cells, or E-selectin bearing L-E cells in a microfluidic parallel-plate flow cell at 1 dyne/cm^2 (18). Cell rolling velocity, rolling cell density, and adherent cell density were quantified as described previously (18, 29).

Statistics—Error bars represent standard deviations (S.D.) for ≥3 independent experiments. Data were analyzed using Student's *t* test for dual comparisons and one-way analysis of variance followed by the Tukey-Kramer test for multiple comparisons. $p < 0.05$ was considered significant.

RESULTS

Expression of Functional PSGL-1 Peptide Probes—PSGL-1 peptide probes, 19FcTM and 76FcTM, were designed to reduce

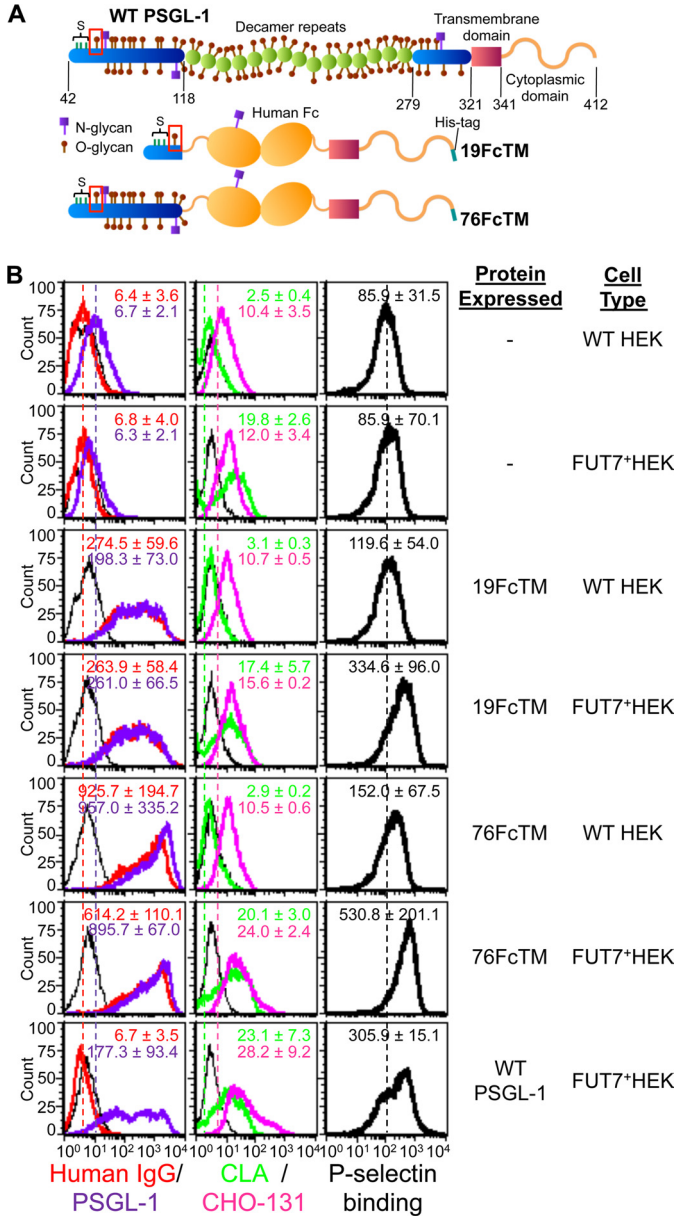

FIGURE 1. **PSGL-1 variants.** *A*, shown is mature PSGL-1 with 73 potential sites for *O*-glycosylation (*brown circles*) and 3 sites for *N*-glycosylation (*purple squares*). N-terminal residues include three sulfated tyrosines (*S*) and a sialofucosylated *O*-glycan at Thr-57 (*red box*). The PSGL-1 variants constructed include either 19 or 76 N-terminal residues followed by the human IgG1 Fc, PSGL-1 transmembrane, and cytoplasmic sections. *B*, HEK293T and FUT7$^+$HEK cells expressing either full-length PSGL-1 or PSGL-1 variants (*19FcTM* and *76FcTM*) were constructed. Flow cytometry histograms characterize anti-human IgG and anti-PSGL-1 mAb KPL-1 binding (*left column*), CLA/HECA-452 and CHO-131 epitope expression (*middle column*), and P-selectin IgG binding (*right column*). Wild-type HEK293T cells do not express PSGL-1. The CLA epitope is augmented upon FUT7 overexpression. Robust P-selectin IgG binding requires co-expression of FUT7 with either wild-type PSGL-1, 19FcTM, or 76FcTM. Numerical values provided in individual histograms represent mean ± S.D. for 4–7 experiments.

the overall *O*-glycan content of the glycoprotein (Fig. 1*A*). In these molecules the *O*-glycan-rich mucinous decamer repeats of native PSGL-1 were replaced with the human IgG1 Fc domain, which lacks *O*-glycans. These probes were expressed as cell-surface glycoproteins via the native PSGL-1 transmembrane and cytoplasmic sections on both normal HEK293T cells (*WT HEK*) and HEK293Ts over-expressing human α(1,3) fucosyltransferase FUT7 (*FUT7$^+$HEK*) (Fig. 1*B*). Cell surface expression was confirmed using both anti-human IgG antibody and anti-PSGL-1 mAb KPL-1 (*first column*). Overexpression of FUT7 in FUT7$^+$HEKs resulted in an 8–10-fold increase in sLe^X expression as measured using the anti-CLA mAb HECA-452 (*second column*). HECA-452 binding was independent of PSGL-1, which suggests the presence of additional glycoconjugates expressing sLe^X other than PSGL-1. In contrast to HECA-452, the CHO-131 epitope was slightly, but reproducibly, elevated only when FUT7 was co-expressed along with either 19FcTM, 76FcTM, or native PSGL-1. These data are consistent with previous work that describes CHO-131 specificity (26). 19FcTM, 76FcTM and native PSGL-1 all bound P-selectin IgG fusion protein at high and comparable levels when expressed in FUT7$^+$HEK293T cells (*last column*). Overall, the PSGL-1 peptide probes containing either the 19 or 76 N-terminal amino acids of PSGL-1 function similarly to the full-length native protein.

O-Glycan Microheterogeneity at the N Terminus of PSGL-1—To determine the *O*-glycan distribution at the PSGL-1 N terminus, lentiviral vectors were developed to express soluble forms of the PSGL-1 peptide probe in hard-to-transfect HL-60 cells (supplemental Table S3). These studies show that EF1α is a superior promoter for stable protein expression in HL-60 compared with phosphoglycerate kinase and CMV. Also, the introduction of the von Willebrand factor signal peptide upstream of the PSGL-1 peptide probe aids expression. Based on this, a viral vector containing the EF1α promoter and a von Willebrand factor signal peptide was developed to drive expression of 19Fc (Fig. 2*A*). This His-tagged protein is similar to 19FcTM (Fig. 1), only it lacks the PSGL-1 transmembrane and cytoplasmic sections.

19Fc was purified from transduced HL-60 using nickel-chelate chromatography. This is a dimeric protein with a monomer mass of 37 kDa under reducing conditions (Fig. 2*B*). The purified protein was detected by Western blotting with both anti-PSGL-1 and anti-human IgG Abs. Protein purity was confirmed using a silver stain. Soluble 19Fc and 19Fc[P62A] were functional as polystyrene beads bearing either glycoprotein bound P-selectin expressing activated platelets efficiently under fluid shear in a cone-plate viscometer assay (Fig. 2*C*). This binding was specifically blocked by anti-PSGL-1 mAb KPL-1, which recognizes the PSGL-1 N terminus. The negative control protein 19Fc[T57A], lacking the Thr-57 *O*-glycan, did not bind platelets.

To confirm that the majority of sialylated *O*-glycans lie within the PSGL-1 N-terminal segment of 19Fc, HL-60 expressing soluble 19Fc were cultured in media containing acetylated *N*-azidoacetylmannosamine. Acetylated *N*-azidoacetylmannosamine introduced in this manner permeates cells, is deacetylated by nonspecific cellular esterases, is converted into an azido form of CMP-sialic acid via bioorthogonal chemistry, and replaces native sialic acid in cellular glycoconjugates (30). A click reaction performed with DBCO-biotin confirmed the metabolic incorporation of azido derivatized sialic acid (SiaNAz) into 19Fc (Fig. 2*D*). Although the enzymatic treatment of 19Fc with either peptide *N*-glycosidase F or EK resulted in a shift in protein mobility, suggesting a loss of molecular mass, only cleavage by EK resulted in the loss of SiaNAz from

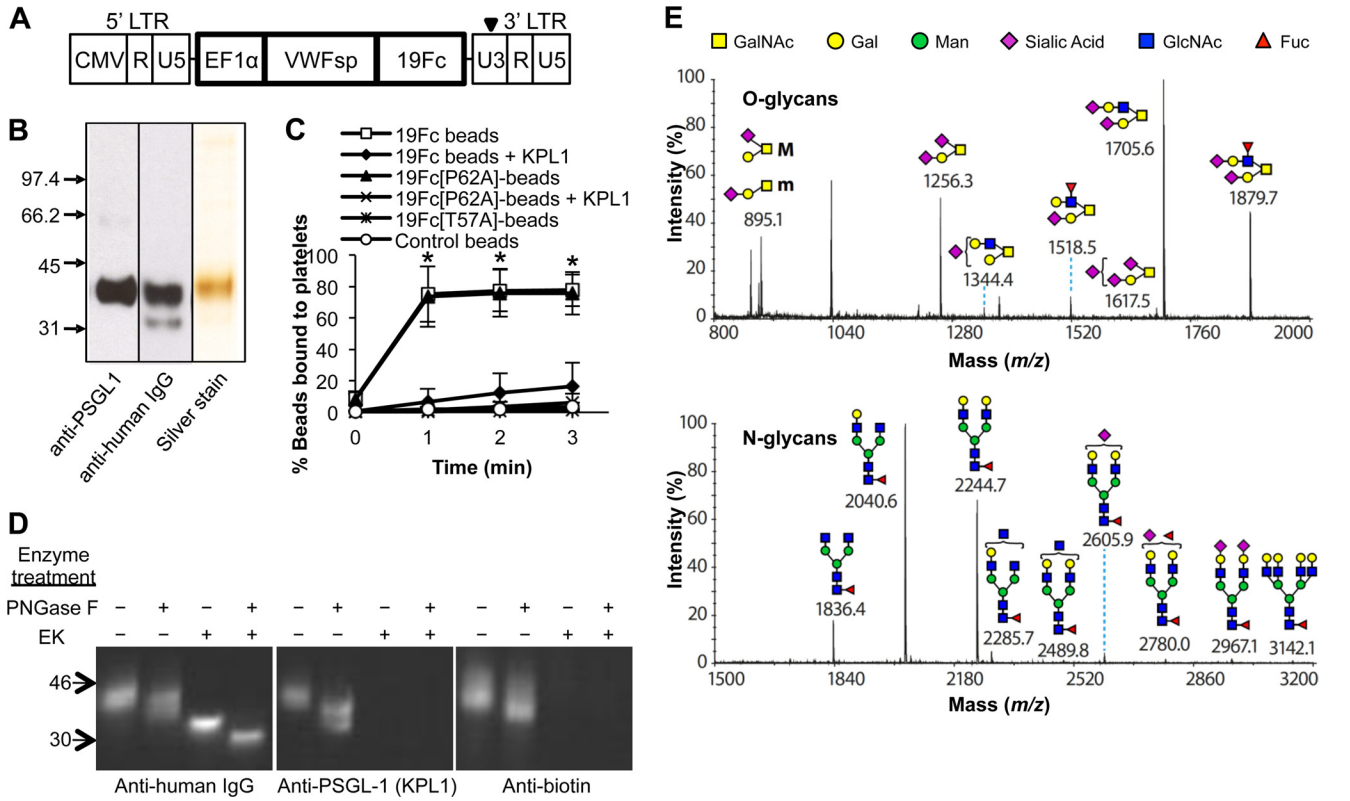

FIGURE 2. **Expression and characterization of 19Fc.** *A*, a lentivirus construct with EF1α promoter and von Willebrand factor signal peptide (*VWFsp*) was used to express soluble 19Fc in HL-60 cells. *R*, repeat; *U*, unique; *LTR*, long terminal repeat. *B*, immunoblotting and silver staining of 19Fc is shown. Western blots used mAb KPL-1 and anti-human IgG for protein detection. *C*, 19Fc beads or negative control 19Fc[T57A] beads were shear-mixed with TRAP-6-activated platelets in a cone-and-plate viscometer at 650/s. % beads with bound platelets was quantified using flow cytometry. Data are the mean ± S.D. for 4–8 experiments. *, $p < 0.001$ with respect to 19Fc/19Fc[P62A] beads treated with mAb KPL-1. *D*, acetylated *N*-azidoacetylmannosamine metabolically incorporated into 19Fc was biotinylated using copper-free DBCO-biotin cycloaddition and detected using anti-biotin Ab in Western blots. Anti-human IgG and anti-PSGL-1 KPL-1 were applied in parallel to follow the C- and N-terminus of 19Fc, respectively. 19Fc digestion with EK resulted in loss of both sialic acid and the 19Fc N-terminus. The only effect of peptide *N*-glycosidase F (*PNGase F*) was on the molecular mass of 19Fc. Thus, a majority of the sialylated glycans of 19Fc reside at the N-terminus. *E*, shown is MALDI-TOF MS analysis of *O*-glycans (*top*) and *N*-glycans (*bottom*) released from 19Fc expressed in HL-60 cells. All molecular ions are $[M+Na]^+$. Putative structures are based on composition, tandem MS, and biosynthetic knowledge. Structures that show sugars *outside of a bracket* have not been unequivocally defined. Prominent *O*-glycan peaks correspond to core-2 sLe^X (*m/z* 1879.7), mono- (*m/z* 895.1), and di- (*m/z* 1256.3) sialylated T-antigen. Major (*M*) and minor (*m*) contributors to peak at *m/z* 895.2 were identified using MALDI-TOF/TOF instrument.

19Fc. Because EK cleaves the PSGL-1 N terminus (supplemental Fig. S1), these data are consistent with the notion that the sialylated *O*-glycans of 19Fc reside exclusively within its N terminus.

MS glycomics analysis of *O*-glycans released from 19Fc demonstrates that 63.8% of the *O*-glycans contain a core-2 structure, whereas the remaining are core-1 based (Fig. 2*E*, Table 1). Two prominent core-2 *O*-glycans were revealed: one bearing the sLe^X epitope (*m/z* 1879.7) and the other displaying a disialylated non-fucosylated glycan (*m/z* 1705.6). Although previous studies that analyzed all *O*-glycans released from full-length PSGL-1 by mild borohydrate treatment suggest that only ~2% of the *O*-glycans contain the non-extended sLe^X structure (Table 1, Refs. 15 and 16), our results demonstrate a relatively high prevalence of this entity at the PSGL-1 N terminus (18% in column 3, Table 1). Furthermore, although the previous reports suggest the presence of extended di- and tri- lactosamine structures on the *O*-glycans of PSGL-1, including those bearing the sLe^X epitope (15, 16), these were absent in 19Fc. With regard to the core-1 glycans, we observed the expression of both the mono- (*m/z* 895.1) and di- (*m/z* 1256.3) sialylated T-antigen structures at the N terminus of PSGL-1. MALDI-TOF/TOF showed that the sialic acid in the mono-sialylated T-antigen is primarily attached to the 6-position of GalNAc rather than the 3-position of Gal (Supplemental Fig. S2). With regard to the *N*-glycans of 19Fc, complex bi-antennary structures with core fucose were most abundant. As anticipated based on Fig. 2*D*, only 4% of these *N*-glycans were sialylated. Overall, important differences were noted between our studies that focus on the *O*-glycans at the PSGL-1 N terminus and previous work that studied all the *O*-glycan of PSGL-1 without focus on site-specific glycosylation (Table 1).

Glycoproteomic Analysis Confirms the Expression of the sLe^X and Di-sialylated T-antigen at Thr-57 of 19Fc—Glycoproteomic analysis was performed to confirm the site-specific localization of O- and *N*-glycans identified in the above glycomics experiment at Thr-57 of PSGL-1 and Asp-144 of the IgG Fc section (Fig. 3). Such experiments utilized both trypsin and Glu-C to digest both 19Fc and 19Fc[P62A], a variant of 19Fc with an additional tryptic digestion site. Enzyme-digested glycopeptides were analyzed using nano-flow chromatography separation coupled to a high resolution tandem MS. Due to the primary amino acid sequence of 19Fc, Glu-C was more efficient when analyzing the *O*-glycans at the PSGL-1 N terminus (Fig. 3,

TABLE 1

***O*-Glycans of PSGL-1**

MALDI-MS analysis on PSGL-1 N terminus (last column) show different *O*-glycan distribution compared with previous *O*-glycan studies on whole PSGL-1 (first and second column). A, absent. Yellow squares, GalNAc; yellow circles, Gal; pink diamonds, sialic acid; blue squares, GlcNAc; red triangles, Fuc.

O-Glycan Structures	Whole PSGL-1		PSGL-1 N-terminus
	Wilkins et al. (16)	Aeed et al. (15)	Current Manuscript
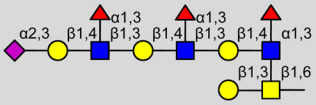	12	A	A
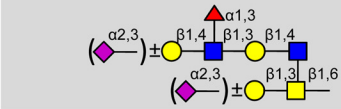	A	2.8	A
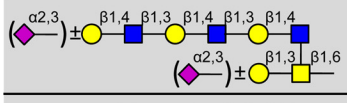	A	3.5	A
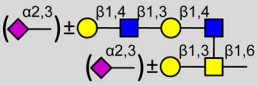	A	6.4	A
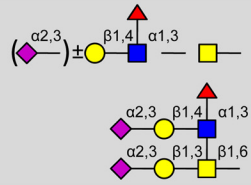	2	1.9	18.0
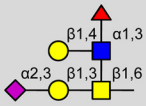	A	A	3.8
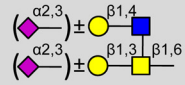	20	45.3	42.0
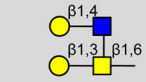	52		A
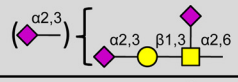	A	A	2.0
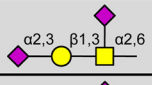	A	A	20.3
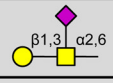	A	A	13.8
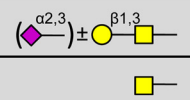	14	36.3	
	A	3.9	A

supplemental Fig. S3), whereas trypsin allowed sequencing of *N*-glycans (supplemental Fig. S4).

MS^2 spectra show the core-2 sLe^X (Fig. 3*A*) and di-sialylated T-antigen (Fig. 3*B*) at Thr-57 of PSGL-1. In both panels, the precursor *m*/*z* was matched within 20 ppm, and the two most intense peaks correspond to a loss of either 1 or 2 sialic acids. Additional high intensity peaks in Fig. 3*A* appear to be due to the loss of either fucose or the entire sLe^X glycan. Glycan signature peaks that indicate the presence of NeuAc (*m*/*z* 292), HexHexNAc (*m*/*z* 366), NeuAcHexHexNAc (*m*/*z* 657), and NeuAcHex(Fuc)HexNac (*m*/*z* 803) also appear. Although glycan fragmentation was generally favored in the collision-induced dissociation mode (supplemental Fig. S4), some peptide breakdown was observed when smaller *O*-glycans with only a few monosaccharides were analyzed. For example, some N-terminal Phe loss accompanies glycan fragmentation in Fig. 3*B*. Together, these studies confirm the presence of *O*-glycans identified by glycomics analysis, including the core-2 sLe^X and di-sialylated T-antigen, at Thr-57 of PSGL-1.

Overexpression of ST6GalNAc2 and -4 in HL-60 Reduces Cell Surface CLA and sLe^X Expression—The prominent sialylation at the 6-position of GalNAc both in the mono- and di-sialylated T-antigen structures suggests a potential contribution of ST6GalNAc-transferases in regulating the relative distribution of core-1 *versus* core-2 *O*-glycans at the N terminus of PSGL-1. To test this hypothesis, ST6GalNAc1, -2, and -4 were overexpressed using lentivirus to create ST6GalNAc1$^+$, 2$^+$, and 4$^+$ HL-60 cells (Fig. 4). Among the six members of the ST6GalNAc-transferase family, these three enzymes act on *O*-glycans, whereas ST6GalNAc3, -5, and -6 are ganglioside-specific (31, 32). Although some reports suggest that ST6GalNAc3 may also sialylate *O*-glycans (32, 33), this enzyme was absent in HL-60, and thus it was not pursued.

Stable expression of ST6GalNAc-transferases in HL-60 led to cells with red fluorescence as the viral vector co-expressed an internal ribosome entry site driven DsRED reporter (Fig. 4*A*). RT-PCR shows that HL-60 expresses moderate levels of ST6GalNAc2 and lower levels of ST6GalNAc1 and -4 (Fig. 4*B*). Overexpression of specific ST6GalNAc-transferases resulted in increased transcript levels of corresponding enzymes (Fig. 4*B*). In comparison to HL-60, mRNA levels of ST6GalNAc2 in primary human neutrophils was higher as determined by quantitative RT-PCR (Fig. 4*C*). ST6GalNAc2$^+$ and ST6GalNAc4$^+$ HL-60 cells express 6.3- and 9.6-fold higher α(2,6) sialyltransferase activity compared with wild-type HL-60s (Fig. 4*D*). Here, as anticipated, the incorporation of radioactive [^{14}C]sialic acid into the α(2,3)-sialylated T-antigen-fetuin substrate was unaffected by the α(2,3)-specific neuraminidase, whereas it was completely released by the *A. ureafaciens* neuraminidase, which recognizes all α(2,3/6/8/9) sialic acid linkages. The substrate used in this study was unable to detect increased ST6GalNAc-transferase activity in the ST6GalNAc1$^+$ HL-60 cells even though this enzyme exhibits similar substrate specificity as ST6GalNAc2 and -4 (32).

Flow cytometry quantified changes in the expression patterns of carbohydrate epitopes as a result of ST6GalNAc overexpression (Fig. 4*E*). Here, PSGL-1, Le^X, and VIM-2 levels were unchanged in the different HL-60 cell lines. However, a marked reduction in CLA/HECA-452 (92–99%) and sLe^X (40–60%) expression was noted in the ST6GalNAc2$^+$ and ST6GalNAc4$^+$ HL-60s. Such a decrease is consistent with the overall hypothesis.

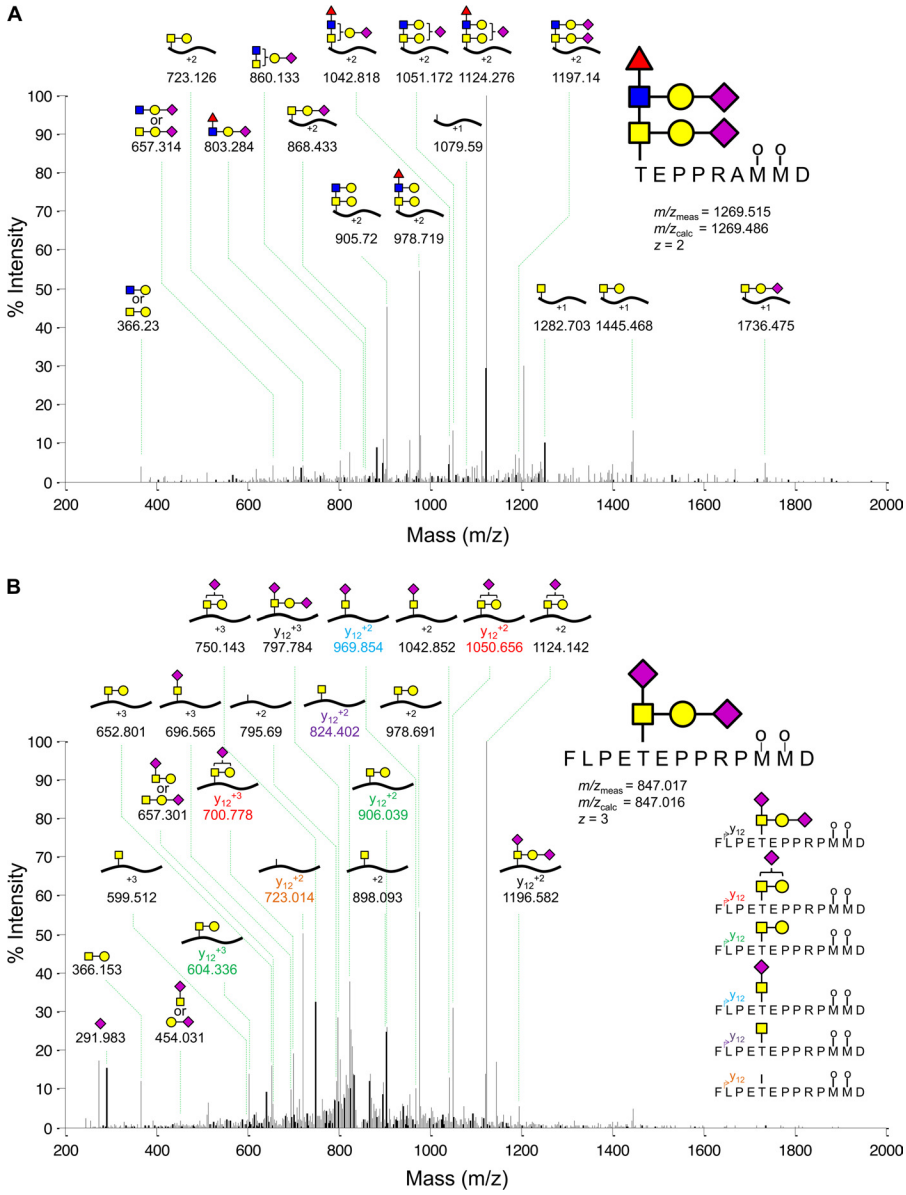

FIGURE 3. **Glycoproteomic analysis.** Core-2 sLe^X (*A*) and di-sialyl T-antigen (*B*) attached to Thr-57 of PSGL-1 was identified in collision-induced dissociation mode. Experimentally measured *m/z* (m/z_{meas}) and theoretically predicted *m/z* (m/z_{calc}) are within 20 ppm. The *top two peaks* in the MS^2 spectra emerge due to loss of sialic acid. Some peaks in *panel B* (shown in color) appear due to loss of N-terminal Phe. *Black curvy lines* used for annotation in both panels indicate the peptide backbone.

Overexpression of ST6GalNAc2 Reduces Leukocyte Adhesion to Activated Platelets—To determine if the reduced expression of CLA/sLe^X on HL-60 impacts the selectin binding function of PSGL-1 (Fig. 5), the various HL-60 cells were shear-mixed with P-selectin expressing activated platelets in a viscometer. ST6GalNAc2$^+$ HL-60 showed a significant reduction in platelet binding at 650/s compared with wild-type HL-60 cells (Fig. 5*A*). ST6GalNAc2$^+$ HL-60s significantly reduced binding to platelets at shear rates from 350 to 4650/s (Fig. 5*B*). Although not statistically significant, a decrease in activated platelet binding to ST6GalNAc4$^+$ HL-60s was noted. Leukocyte-platelet binding under these experimental conditions is exclusively mediated by P-selectin-PSGL-1 binding as it is abrogated by mAbs against either antigens (Fig. 5, Ref. 28).

ST6GalNAc2$^+$ HL-60 Cells Exhibit Reduced Rolling on P-and L-selectin but Not E-selectin under Fluid Shear—Microfluidics-based cell adhesion studies were undertaken to confirm the reduction in PSGL-1 binding upon overexpression of the ST6GalNAc-transferases (Fig. 6). Such studies were performed on substrates composed of either P-selectin-bearing CHO-P cells (Fig. 6, *A* and *B*), immobilized recombinant L-selectin (Fig. 6, *C* and *D*), or E-selectin bearing L-E cells (Fig. 6, *E* and *F*). Here, the anti-PSGL-1 mAb KPL-1 blocked 98, 86, and 37% of leukocyte binding to P- (Fig. 6*A*), L- (Fig. 6*C*), and E-selectin (Fig. 6*E*), respectively. ST6GalNAc2$^+$ HL-60 displayed ~85% reduction in rolling cell density on both P- (Fig. 6*A*, supplemental Movie A) and L-selectin (Fig. 6*C*). The median rolling velocity of residual rolling ST6GalNAc2$^+$ HL-60 cells on P- and L-selectin was also increased ~2-fold compared with wild-type HL-60s. A modest reduction in cell rolling density and increase in cell rolling velocity was also observed during ST6GalNAc1$^+$ and 4$^+$ HL-60s rolling on L-selectin, although this was less remarkable compared with the ST6GalNAc2$^+$ HL-60 cells (Fig. 6, *C* and *D*).

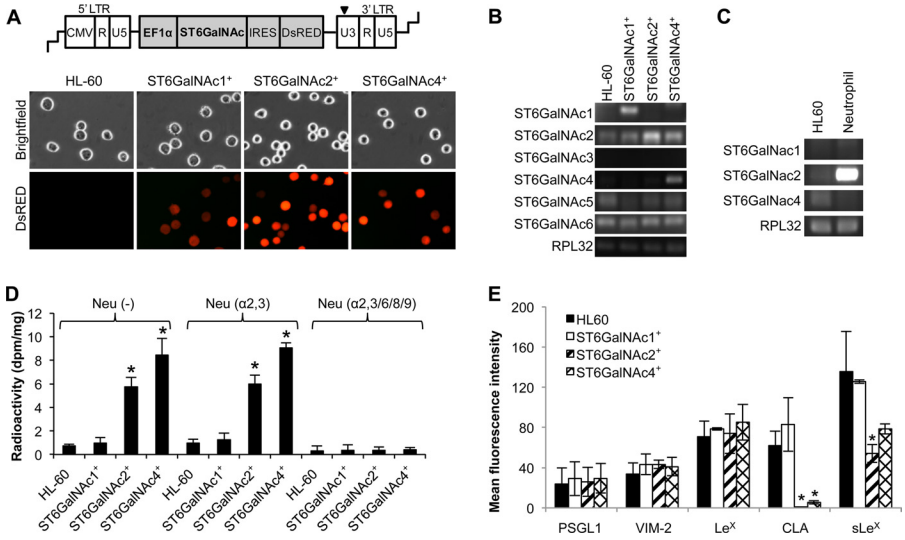

FIGURE 4. **Overexpression of ST6GalNAc1, -2, and -4 in HL-60.** *A*, lentivirus vector used to overexpress ST6GalNAc-transferases in HL-60 co-expressed a DsRED (red fluorescent protein) reporter. Micrographs show DsRED expression in all transduced HL-60s. *IRES*, internal ribosome entry site. *B*, RT-PCR analysis of ST6GalNAc-transferases in wild-type HL-60 and HL-60s overexpressing ST6GalNAc-transferases is shown. RT-PCR products were resolved on an agarose gel and sequence-verified. *C*, shown is an RT-PCR comparison of ST6GalNAc-transferase expression in HL-60 *versus* human peripheral blood neutrophils. *D*, ST6GalNAc-transferase activity in various HL-60 cell lysates was measured by detecting [^{14}C]NeuAc incorporation into α(2,3)-sialylated fetuin substrate. Incorporated radioactivity was released by α(2,3/6/8/9) *A. ureafaciens* neuraminidase but not α(2,3) *M. decora* neuraminidase. *, $p < 0.001$ compared with normal HL-60. *E*, cell surface expression of PSGL-1 (KPL-1), CD65s/VIM-2, CD15/Le^X (HI98), CLA (HECA-452), and CD15s/sLe^X (CSLEX-1) on HL-60 and its variants is shown. ST6GalNAc2 and ST6GalNAc4 overexpression reduced CLA/HECA-452 expression with ST6GalNAc2 also reducing the sLe^X/CSLEX-1 epitope. Data are the mean ± S.D. for 3–5 experiments. *, $p < 0.001$ compared with normal HL-60.

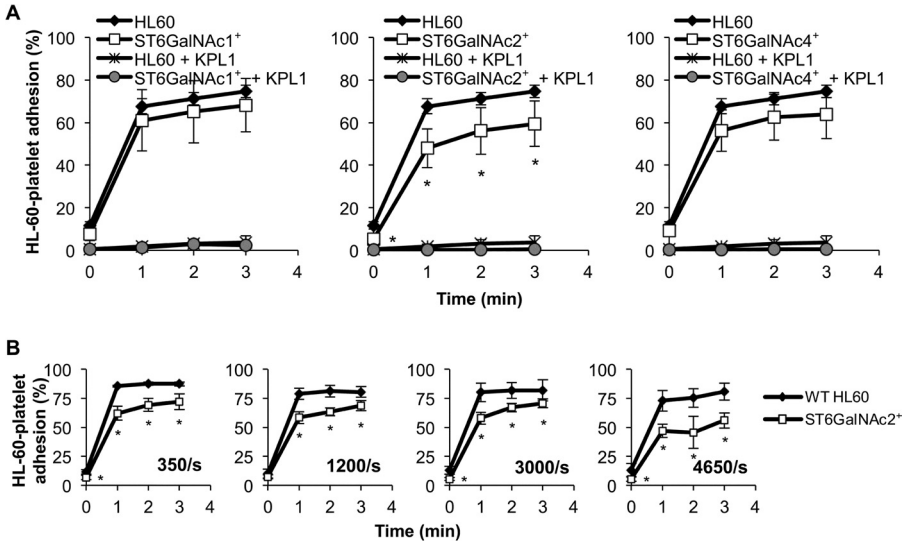

FIGURE 5. **PSGL-1-dependent HL-60 binding to activated platelets.** *A*, wild-type HL-60 or ST6GalNAc1$^+$/2$^+$/4$^+$ HL-60 cells were sheared with TRAP-6-activated platelets at 650/s. Cell-platelet heterotypic binding was blocked by anti-PSGL-1 mAb KPL-1. ST6GalNAc2$^+$ HL-60 cells displayed decreased adhesion to activated platelets compared with wild-type HL-60. *B*, reduced ST6GalNAc2$^+$ HL-60 platelet binding was observed at all shear rates. Data are the mean ± S.D. from 5–11 experiments. *, $p < 0.05$ with respect to wild-type HL-60.

ST6GalNAc-transferase overexpression had a modest effect on leukocyte rolling on E-selectin. Here, a ~67% reduction in the number of adherent cells was observed with ST6GalNAc2$^+$ and ST6GalNAc4$^+$ HL-60s, although this treatment also resulted in higher rolling cell densities (Fig. 6*E*). ST6GalNAc2 and ST6GalNAc4 overexpression also doubled cell rolling velocity compared with wild-type HL-60s (Fig. 6*F*). The smaller effect of ST6GalNAc2 on E-selectin-mediated cell adhesion, compared with L- and P-selectin, indicates that the balance between sLe^X and di-sialyl T-antigen synthesis may not be critical for selectin ligands other than PSGL-1.

19Fc Expressed in ST6GalNAc2$^+$ HL-60s Display Reduced sLe^X Expression and P-selectin Binding—19Fc was expressed in ST6GalNAc2$^+$ HL-60s (19Fc[ST6GalNAc2$^+$]) to determine the effect of this enzyme on core-2 sLe^X *O*-glycan synthesis (Fig. 7). Here, consistent with the whole cell measurements, 19Fc[ST6GalNAc2$^+$] displayed lower levels of core-2 sLe^X (*m*/*z* 1879.7) and higher levels of the di-sialylated T-antigen (*m*/*z* 1705.6) compared with 19Fc (Fig. 7*A* *versus* Fig. 2*D*). High levels of the di-sialylated core-2 structure were also detected, and the reason for this is unclear. ST6GalNAc-transferase overexpression did not alter HL-60 α(1,3)fucosyltransferase activity as

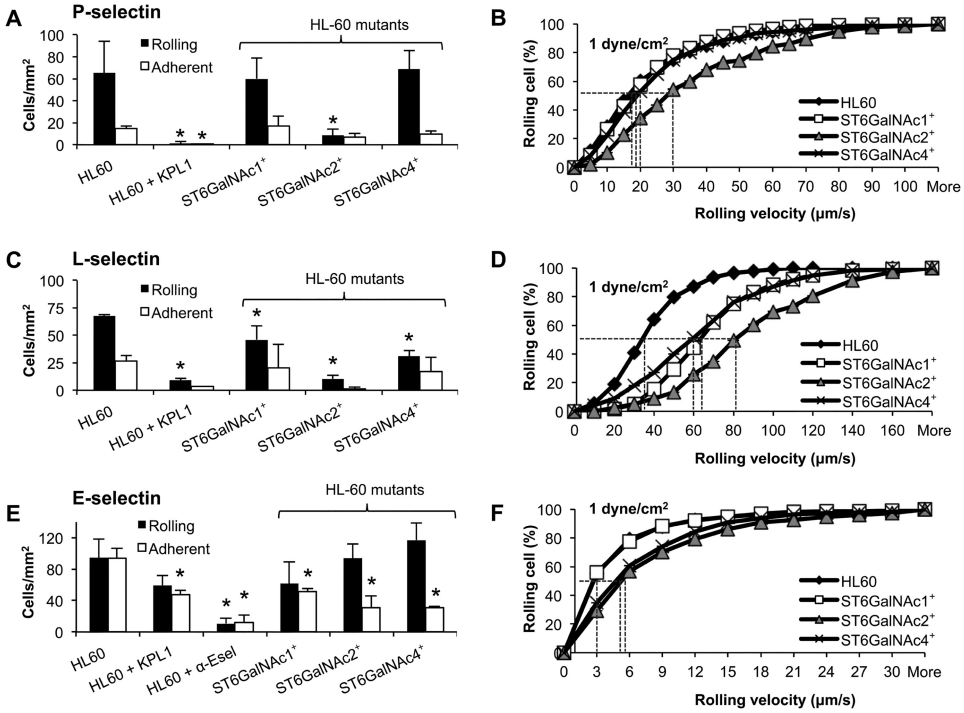

FIGURE 6. **HL-60 rolling on selectin bearing substrates.** Wild-type HL-60 or cells overexpressing ST6GalNAc-transferases were perfused over CHO-P cells (*A* and *B*) recombinant L-selectin (*C* and *D*), and E-selectin bearing L-cells (*E* and *F*) at a wall shear stress of 1 dyn/cm^2. The number of rolling cells, adherent cells, and cell rolling velocity was quantified. ST6GalNAc2$^+$ cells displayed ~85% reduction in rolling cell density and a 1.8–2.5-fold increase in cell rolling velocity on P- and L-selectin substrates compared with wild-type HL-60. ST6GalNAc1 and -4 overexpression also reduced leukocyte rolling density and increased cell rolling velocity on L-selectin. ST6GalNAc-transferase overexpression had a relatively small effect on E-selectin-dependent cell adhesion. Data are the mean ± S.D. from 3–4 experiments. *, $p < 0.05$ with respect to wild-type HL-60.

measured using N-acetyllactosamine (Galβ1,4 GlcNAc), sialyllactosamine (NeuAcα2,3Galβ1,4 GlcNAc), and core-2 tetrasaccharide (Galβ1,3(Galβ1,4GlcNAcβ1,6)GalNAc) based synthetic substrates (data not shown).

19Fc[ST6GalNAc2$^+$] immobilized on polystyrene beads bound activated platelets at 75% lower levels compared with beads having the same amount of immobilized 19Fc (Fig. 7*B*). Together, the data demonstrate that ST6GalNAc2 can regulate the balance between the expression of the core-2 sLe^X epitope and the di-sialylated T-antigen glycan at the N terminus of PSGL-1.

Partial Co-localization of ST6GalNAc2 and C2GnT-1—In leukocytes the effective competition between sLe^X formation on the core-2 *O*-glycan and di-sialyl T-antigen synthesis requires the co-localization of ST6GalNAc2 with core-2 GlcNAc-transferase C2GnT-1 (Fig. 8). To determine if this is the case, two fusion proteins ST6GalNAc2-DsRED and C2GnT-1-EGFP, both carrying distinct fluorescence reporters, were transduced into HEK293T cells (Fig. 8*A*). Consistent with this proposition, partial co-localization of the enzymes with an overlap coefficient of 0.816 was observed (Fig. 8*A*, supplemental Movie B). Confocal microscopy studies with negative control samples, wild-type HEK293T, and HEK293Ts individually transduced with either ST6GalNAc2-DsRED or C2GnT-1-EGFP alone confirm the absence of signal leakage between the instrument DsRED and EGFP signal channels (supplemental Fig. S5).

DISCUSSION

Glycan Microheterogeneity at the N Terminus of PSGL-1—This study introduces methods to quantitatively measure site-specific *O*-linked glycosylation with focus on the glycan heterogeneity at Thr-57 of PSGL-1. To this end, "peptide probes," which lack the PSGL-1 mucinous decamer repeat section, were created. Protein expression in human leukocyte HL-60 cells was optimized by varying promoter and signal peptide sequences. High levels of protein production were noted upon using lentivirus containing the EF1α promoter and von Willebrand factor signal peptide.

Among the peptide probes, detailed investigations were performed with 19Fc as it contains the minimal PSGL-1 peptide sequence necessary to bind selectins under shear flow. The sialylated glycans of 19Fc were almost exclusively located at the N terminus of this protein. MALDI-TOF MS analysis of the *O*-glycans released from 19Fc quantified the glycan microheterogeneity at the PSGL-1 N terminus. Glycoproteomic analysis using LC-MS/MS confirmed that the glycans identified using MALDI-TOF MS were located at Thr-57 of PSGL-1. Besides studying native *O*-glycans, this approach also allowed investigation of glycan structural changes in 19Fc upon perturbation of cellular glycosyltransferases.

The study confirms the existence of a core-2 based sialyl Lewis-X glycan (*m*/*z* 1879.7) at Thr-57 as predicted by prior work (11). It also revealed the existence of α(2,6) sialylated glycans including the mono- (Galβ1,3(NeuAcα2,6) GalNAc; *m*/*z* 895.1) and di- (NeuAcα2,3Galβ1,3 (NeuAcα2,6)GalNAc, *m*/*z* 1256.3) sialylated T-antigens at this position. Although similar structures have been observed during whole cell *O*-glycome analysis of a variety of PSGL-1 bearing cells including monocytes, dendritic cells, and neutrophils (34, 35), this is the first

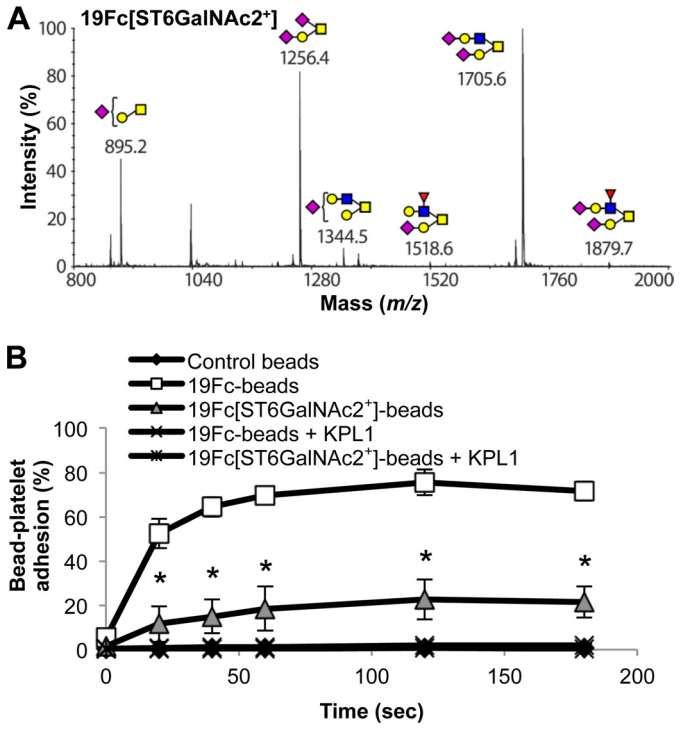

FIGURE 7. **Characterization of 19Fc purified from ST6GalNAc2$^+$ HL-60 (19Fc[ST6GalNAc2$^+$]).** *A*, MALDI-TOF MS spectra show marked reduction in the core-2 sLe^X structure on 19Fc[ST6GalNAc2$^+$] compared with 19Fc (Fig. 2*D*). All molecular ions are [M+Na]$^+$. Putative structures are based on composition, tandem MS, and biosynthetic knowledge. Structures that show sugars outside of a *bracket* have not been unequivocally defined. *B*, 19Fc or 19Fc[ST6GalNAc2$^+$] beads were shear mixed in a viscometer with activated platelets following the protocol outlined in Fig. 2*C*. 19Fc[ST6GalNAc2$^+$] beads displayed a reduced capacity to bind platelets compared with 19Fc beads. *, $p < 0.001$ with respect to 19Fc beads.

report of the expression of such glycans at the N terminus of PSGL-1.

There are three potential reasons why α(2,6)-sialylated glycans may have been missed in previous studies that characterized the *O*-glycans of PSGL-1 (15, 16). (i) The prior work applied Newcastle disease virus neuraminidase to rule out the presence of α(2,6)-sialylated glycans. In this context, whereas the Newcastle disease virus sialidase has high specificity for α(2,3) linkages (36), it also cleaves α(2,6) sialic acid linked to GalNAc, albeit at slower rates, if a sugar is β(1,3)-linked to GalNAc (37). Examples of such Newcastle disease virus neuraminidase-cleavable substrates include Galβ1,3(NeuAcα2,6)GalNAc and NeuAcα2,3Galβ1,3-(NeuAcα2,6)GalNAc (37). (ii) The previous studies examined all the *O*-glycans of PSGL-1 without specific focus on Thr-57 at the N terminus (15, 16). Due to the abundance of *O*-glycans in the mucinous decamer repeat section of PSGL-1, these studies more likely revealed the glycan distribution in this section rather than at the functional N terminus. Thus, it may be that the α(2,6)-sialylated glycan is prominently expressed only at the N terminus. (iii) The previous work applied conventional lectin-based recognition and chromatography methods unlike the current study that relies on ultra-high sensitive mass spectrometry. Differences in sample preparation and detection methods may account for the different observations.

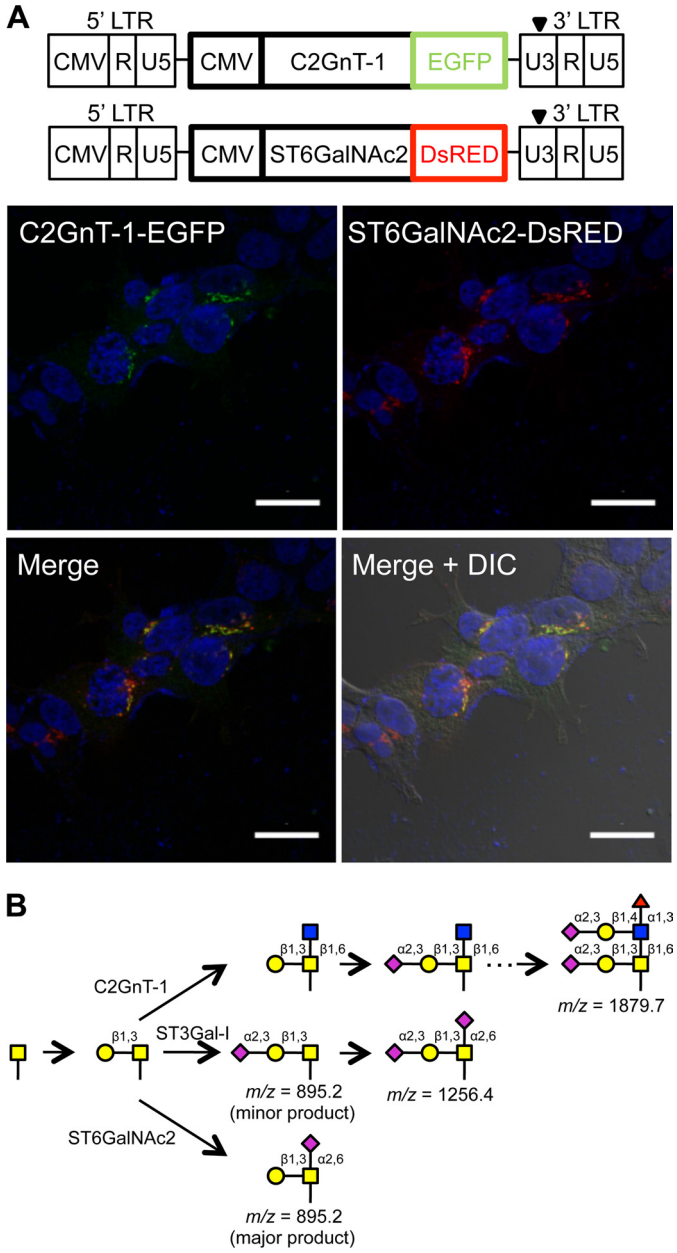

FIGURE 8. **Co-localization of ST6GalNAc2 and C2GnT-1.** *A*, HEK293T cells were transduced with virus encoding for full-length C2GnT-1-EGFP and ST6GalNAc2-DsRED fusion proteins. Partial co-localization is noted (*yellow regions in the merged image*) in the confocal microscope image. *Scale bar* = 20 μm. *B*, the model suggests competition between ST3Gal-I, ST6GalNAc2, and C2GnT-1 for the T-antigen/core-1 substrate Galβ1,3GalNAc. *DIC*, differential interference contrast.

A Potential Role for ST6GalNAc2 in Regulating Leukocyte Adhesion—The current study suggests that the ST6GalNAc-transferases can regulate leukocyte sLe^X biosynthesis and L-/P-selectin-dependent cell adhesion. Among the members of this enzyme family, our data support a potential role for ST6GalNAc2 in human neutrophils as this enzyme is expressed in these cells. Overexpression of ST6GalNAc2 in HL-60 reduced cell surface sLe^X expression, diminished cell adhesion to P-selectin bearing activated human platelets, and caused reduced cell rolling on substrates bearing P- and L-selectin. The effect of ST6GalNAc2 overexpression on E-selectin binding function was less dramatic with only a modest reduction in the

number of adherent cells. Expression of 19Fc in ST6GalNAc2$^+$ HL-60 also resulted in the near complete loss of the core-2 sLe^X glycan at the PSGL-1 N terminus.

In addition to ST6GalNAc2, ST6GalNAc4 overexpression also resulted in a decrease in cell surface CLA/HECA-452 expression, although the impact of this perturbation on P- and L-selectin-dependent cell rolling was small compared with ST6GalNAc2. One possible explanation is that although both ST6GalNAc2 and ST6GalNAc4 sialylate a variety of *O*-glycans on leukocytes, the PSGL-1 N terminus may only be a preferred substrate for ST6GalNAc2. Due to this, an overall reduction in cell surface HECA-452 expression may not correlate with selectin binding function. Consistent with this proposition, a previous study reports the existence of sLe^X-deficient HL60 variants that exhibit high levels of adhesion to both E- and P-selectin (38). Whether ST6GalNAc-transferase activity is altered in these cells remains unknown.

The Balance between Core-2 Sialyl Lewis-X and Di-sialylated T-antigen—A competition between three enzymes, C2GnT-1, ST3Gal-I, and ST6GalNAc2, for their common T-antigen/Galβ1,3GalNAc substrate may regulate the relative distribution of the core-2 sLe^X and di-sialylated T-antigen structures at the PSGL-1 N terminus (Fig. 8*B*). First, with regard to the competition between C2GnT-1 and ST3Gal-I, a partial co-localization of both enzymes in the medial-Golgi is reported (39, 40). Additionally, Whitehouse *et al.* (40) demonstrate that ST3Gal-I overexpression in breast cancer cells inhibits the development of core-2-based *O*-glycans. Using mice, Priatel *et al.* (41) also show that knocking out ST3Gal-I results in an increase in core-2 *O*-glycan expression even though C2GnT enzyme activity remains unchanged. Together, these data suggest that the synthesis of the α(2,3)-sialylated core-1 epitope by ST3Gal-I may result in a substrate that is not acted upon efficiently by the C2GnTs. Second, the competition between C2GnT-1 and ST6GalNAc2 is supported by our confocal microscopy observation that these enzymes partially co-localize in the Golgi. In addition, the effect of ST6GalNAc2 overexpression in the current study is similar to the effect of knocking out C2GnT-1 in a mouse model (42, 43). In both cases leukocytes overexpressing ST6GalNAc2 or lacking C2GnT-1 display a dramatic reduction in their ability to bind immobilized L- and P-selectin, whereas their binding to E-selectin is only mildly altered. Finally, our MS data demonstrating a higher prevalence of α(2,6)- rather than α(2,3)-sialylated core-1 glycans at *m*/*z* 895 indicate a potential competition between ST6GalNAc2 and ST3Gal-1. In this regard, although ST3Gal-1 efficiently sialylates the core-2 trisaccharide Galβ1,3(GlcNAcβ1,6)GalNAc, this enzyme shows poor activity toward Galβ1,3(NeuAcα2,6)GalNAc, a substrate formed by the action of ST6GalNAc2 on the T-antigen substrate.

In addition to selectin-mediated granulocyte adhesion, the balance between C2GnT-1 and ST6GalNAc-transferase activities may also regulate T-cell and dendritic cell function. In this context, T-cell activation is accompanied by a coordinated decrease in ST6GalNAc-transferase and a dramatic up-regulation of core-2 β(1,6)GlcNAc- and α(1,3)fucosyl-transferase activity (44, 45). As a result, a shift in glycan structures may be expected from the di-sialylated T-antigen in naïve T-cells to core-2 sLe^X upon T-cell activation. Based on the current work, this transition may occur at the PSGL-1 N terminus. In naïve T-cells, the smaller di-sialylated T-antigen at the PSGL-1 N terminus may allow the binding of chemokines (CCL19, CCL21, and CCL27) to tyrosine sulfation residues at the N terminus of PSGL-1, thereby facilitating lymphocyte homing to secondary lymphoid organs (4, 46, 47). After activation, the shift to the larger core-2 sLe^X glycan may both sterically reduce chemokine binding to PSGL-1 and simultaneously enhance cell adhesion to selectins that are expressed at sites of inflammation (46). In this model the competition between ST6GalNAc-transferases and C2GnT-1 for the T-antigen substrate at the N terminus of PSGL-1 regulates both naïve T-cell homing to secondary lymphoid organs and effector T-cell targeting to sites of inflammation (4, 46).

In the case of dendritic cells, maturation is accompanied by a decrease in C2GnT-1 and an increase in ST6GalNAc2 transcript levels (34). Based on the current work, a transition from the core-2 sLe^X glycan to the di-sialylated T-antigen may be expected at the PSGL-1 N terminus. Such changes in the *O*-glycan profile may regulate the transition of immature dendritic cell migration pattern from a PSGL-1/sLe^X-dependent mechanism that targets inflamed tissue to a PSGL-1-independent migration to lymph nodes after maturation (48).

In conclusion, this manuscript introduces new tools to study site-specific glycosylation. It demonstrates the existence of a di-sialylated T-antigen glycan at Thr-57 of PSGL-1 and suggests a potential role for ST6GalNAc2 in regulating the balance between the di-sialylated T-antigen and the core-2 sLe^X glycan at this position. This balance may impact the cell adhesion phenotype of granulocytes and additional leukocyte subpopulations. Whereas the current study relies on gene overexpression, additional studies where ST6GalNAc2 is either knocked down in human cells or deleted in mice can strengthen the potential role of this enzyme. Indeed mice lacking ST6GalNAc2 have recently been created in a 129 parental background, and these animals display reduced body weight and B-cell proliferation defects (49). The leukocyte selectin-dependent adhesion function is yet unreported, although this is worth investigating.

Acknowledgments—We thank Drs. Shilpa A. Patil and Alexander Buffone Jr. for providing some of the plasmid vectors used in this work.

REFERENCES

1. Moore, K. L., Stults, N. L., Diaz, S., Smith, D. F., Cummings, R. D., Varki, A., and McEver, R. P. (1992) Identification of a specific glycoprotein ligand for P-selectin (Cd62) on myeloid cells. *J. Cell Biol.* **118,** 445–456
2. Sako, D., Chang, X. J., Barone, K. M., Vachino, G., White, H. M., Shaw, G., Veldman, G. M., Bean, K. M., Ahern, T. J., and Furie, B. (1993) Expression cloning of a functional glycoprotein ligand for P-selectin. *Cell* **75,** 1179–1186
3. Patel, K. D., Moore, K. L., Nollert, M. U., and McEver, R. P. (1995) Neutrophils use both shared and distinct mechanisms to adhere to selectins under static and flow conditions. *J. Clin. Invest.* **96,** 1887–1896
4. Veerman, K. M., Williams, M. J., Uchimura, K., Singer, M. S., Merzaban, J. S., Naus, S., Carlow, D. A., Owen, P., Rivera-Nieves, J., Rosen, S. D., and Ziltener, H. J. (2007) Interaction of the selectin ligand PSGL-1 with chemokines CCL21 and CCL19 facilitates efficient homing of T cells to secondary lymphoid organs. *Nat. Immunol.* **8,** 532–539

5. Rossi, F. M., Corbel, S. Y., Merzaban, J. S., Carlow, D. A., Gossens, K., Duenas, J., So, L., Yi, L., and Ziltener, H. J. (2005) Recruitment of adult thymic progenitors is regulated by P-selectin and its ligand PSGL-1. *Nat. Immunol.* **6,** 626–634
6. McEver, R. P., and Cummings, R. D. (1997) Perspectives series. Cell adhesion in vascular biology. Role of PSGL-1 binding to selectins in leukocyte recruitment. *J. Clin. Invest.* **100,** 485–491
7. Afshar-Kharghan, V., Diz-Küçükkaya, R., Ludwig, E. H., Marian, A. J., and López, J. A. (2001) Human polymorphism of P-selectin glycoprotein ligand 1 attributable to variable numbers of tandem decameric repeats in the mucinlike region. *Blood* **97,** 3306–3307
8. Veldman, G. M., Bean, K. M., Cumming, D. A., Eddy, R. L., Sait, S. N., and Shows, T. B. (1995) Genomic organization and chromosomal localization of the gene encoding human P-selectin glycoprotein ligand. *J. Biol. Chem.* **270,** 16470–16475
9. Goetz, D. J., Greif, D. M., Ding, H., Camphausen, R. T., Howes, S., Comess, K. M., Snapp, K. R., Kansas, G. S., and Luscinskas, F. W. (1997) Isolated P-selectin glycoprotein ligand-1 dynamic adhesion to P- and E-selectin. *J. Cell Biol.* **137,** 509–519
10. Liu, W., Ramachandran, V., Kang, J., Kishimoto, T. K., Cummings, R. D., and McEver, R. P. (1998) Identification of N-terminal residues on P-selectin glycoprotein ligand-1 required for binding to P-selectin. *J. Biol. Chem.* **273,** 7078–7087
11. Foxall, C., Watson, S. R., Dowbenko, D., Fennie, C., Lasky, L. A., Kiso, M., Hasegawa, A., Asa, D., and Brandley, B. K. (1992) The three members of the selectin receptor family recognize a common carbohydrate epitope, the sialyl Lewis(x) oligosaccharide. *J. Cell Biol.* **117,** 895–902
12. Li, F., Wilkins, P. P., Crawley, S., Weinstein, J., Cummings, R. D., and McEver, R. P. (1996) Post-translational modifications of recombinant P-selectin glycoprotein ligand-1 required for binding to P- and E-selectin. *J. Biol. Chem.* **271,** 3255–3264
13. Pouyani, T., and Seed, B. (1995) Psgl-1 recognition of P-selectin is controlled by a tyrosine sulfation consensus at the Psgl-1 amino terminus. *Cell* **83,** 333–343
14. Sako, D., Comess, K. M., Barone, K. M., Camphausen, R. T., Cumming, D. A., and Shaw, G. D. (1995) A sulfated peptide segment at the amino terminus of Psgl-1 is critical for P-selectin binding. *Cell* **83,** 323–331
15. Aeed, P. A., Geng, J. G., Asa, D., Raycroft, L., Ma, L., and Elhammer, A. P. (1998) Characterization of the *O*-linked oligosaccharide structures on P-selectin glycoprotein ligand-1 (PSGL-1). *Glycoconj. J.* **15,** 975–985
16. Wilkins, P. P., McEver, R. P., and Cummings, R. D. (1996) Structures of the *O*-glycans on P-selectin glycoprotein ligand-1 from HL-60 cells. *J. Biol. Chem.* **271,** 18732–18742
17. Marathe, D. D., Chandrasekaran, E. V., Lau, J. T., Matta, K. L., and Neelamegham, S. (2008) Systems-level studies of glycosyltransferase gene expression and enzyme activity that are associated with the selectin binding function of human leukocytes. *FASEB J.* **22,** 4154–4167
18. Buffone, A., Jr., Mondal, N., Gupta, R., McHugh, K. P., Lau, J. T., and Neelamegham, S. (2013) Silencing α1,3-fucosyltransferases in human leukocytes reveals a role for FUT9 enzyme during E-selectin-mediated cell adhesion. *J. Biol. Chem.* **288,** 1620–1633
19. Jayakumar, D., Marathe, D. D., and Neelamegham, S. (2009) Detection of site-specific glycosylation in proteins using flow cytometry. *Cytometry A* **75,** 866–873
20. Jang-Lee, J., North, S. J., Sutton-Smith, M., Goldberg, D., Panico, M., Morris, H., Haslam, S., and Dell, A. (2006) Glycomic profiling of cells and tissues by mass spectrometry. Fingerprinting and sequencing methodologies. *Methods Enzymol.* **415,** 59–86
21. Ceroni, A., Maass, K., Geyer, H., Geyer, R., Dell, A., and Haslam, S. M. (2008) GlycoWorkbench. A tool for the computer-assisted annotation of mass spectra of glycans. *J. Proteome Res.* **7,** 1650–1659
22. Eng, J. K., Mccormack, A. L., and Yates, J. R. (1994) An Approach to correlate tandem mass-spectral data of peptides with amino acid sequences in a protein database. *J. Am. Soc. Mass Spectrom.* **5,** 976–989
23. Meng, F., Cargile, B. J., Miller, L. M., Forbes, A. J., Johnson, J. R., and Kelleher, N. L. (2001) Informatics and multiplexing of intact protein identification in bacteria and the archaea. *Nat. Biotechnol.* **19,** 952–957
24. Patil, S. A., Chandrasekaran, E. V., Matta, K. L., Parikh, A., Tzanakakis, E. S., and Neelamegham, S. (2012) Scaling down the size and increasing the throughput of glycosyltransferase assays. Activity changes on stem cell differentiation. *Anal. Biochem.* **425,** 135–144
25. Bolte, S., and Cordelières, F. P. (2006) A guided tour into subcellular colocalization analysis in light microscopy. *J. Microsc.* **224,** 213–232
26. Walcheck, B., Leppanen, A., Cummings, R. D., Knibbs, R. N., Stoolman, L. M., Alexander, S. R., Mattila, P. E., and McEver, R. P. (2002) The monoclonal antibody CHO-131 binds to a core 2 *O*-glycan terminated with sialyl-Lewis x, which is a functional glycan ligand for P-selectin. *Blood* **99,** 4063–4069
27. Beauharnois, M. E., Lindquist, K. C., Marathe, D., Vanderslice, P., Xia, J., Matta, K. L., and Neelamegham, S. (2005) Affinity and kinetics of sialyl Lewis-X and core-2 based oligosaccharides binding to L- and P-selectin. *Biochemistry* **44,** 9507–9519
28. Xiao, Z., Goldsmith, H. L., McIntosh, F. A., Shankaran, H., and Neelamegham, S. (2006) Biomechanics of P-selectin PSGL-1 bonds. Shear threshold and integrin-independent cell adhesion. *Biophys. J.* **90,** 2221–2234
29. Marathe, D. D., Buffone, A., Jr., Chandrasekaran, E. V., Xue, J., Locke, R. D., Nasirikenari, M., Lau, J. T., Matta, K. L., and Neelamegham, S. (2010) Fluorinated per-acetylated GalNAc metabolically alters glycan structures on leukocyte PSGL-1 and reduces cell binding to selectins. *Blood* **115,** 1303–1312
30. Saxon, E., and Bertozzi, C. R. (2000) Cell surface engineering by a modified Staudinger reaction. *Science* **287,** 2007–2010
31. Harduin-Lepers, A., Vallejo-Ruiz, V., Krzewinski-Recchi, M. A., Samyn-Petit, B., Julien, S., and Delannoy, P. (2001) The human sialyltransferase family. *Biochimie* **83,** 727–737
32. Kono, M., Tsuda, T., Ogata, S., Takashima, S., Liu, H., Hamamoto, T., Itzkowitz, S. H., Nishimura, S., and Tsuji, S. (2000) Redefined substrate specificity of ST6GalNAc II. A second candidate sialyl-Tn synthase. *Biochem. Biophys. Res. Commun.* **272,** 94–97
33. Tsuchida, A., Ogiso, M., Nakamura, Y., Kiso, M., and Furukawa, K. (2005) Molecular cloning and expression of human ST6GalNAc III. Restricted tissue distribution and substrate specificity. *J. Biochem.* **138,** 237–243
34. Julien, S., Grimshaw, M. J., Sutton-Smith, M., Coleman, J., Morris, H. R., Dell, A., Taylor-Papadimitriou, J., and Burchell, J. M. (2007) Sialyl-Lewis(x) on P-selectin glycoprotein ligand-1 is regulated during differentiation and maturation of dendritic cells. A mechanism involving the glycosyltransferases C2GnT1 and ST3Gal I. *J. Immunol.* **179,** 5701–5710
35. Babu, P., North, S. J., Jang-Lee, J., Chalabi, S., Mackerness, K., Stowell, S. R., Cummings, R. D., Rankin, S., Dell, A., and Haslam, S. M. (2009) Structural characterization of neutrophil glycans by ultra sensitive mass spectrometric glycomics methodology. *Glycoconj. J.* **26,** 975–986
36. Paulson, J. C., Weinstein, J., Dorland, L., van Halbeek, H., and Vliegenthart, J. F. (1982) Newcastle disease virus contains a linkage-specific glycoprotein sialidase. Application to the localization of sialic acid residues in *N*-linked oligosaccharides of α1-acid glycoprotein. *J. Biol. Chem.* **257,** 12734–12738
37. Amano, J., Nishimura, R., Mochizuki, M., and Kobata, A. (1988) Comparative study of the mucin-type sugar chains of human chorionic gonadotropin present in the urine of patients with trophoblastic diseases and healthy pregnant women. *J. Biol. Chem.* **263,** 1157–1165
38. Wagers, A. J., Stoolman, L. M., Craig, R., Knibbs, R. N., and Kansas, G. S. (1998) An sLex-deficient variant of HL60 cells exhibits high levels of adhesion to vascular selectins. Further evidence that HECA-452 and CSLEX1 monoclonal antibody epitopes are not essential for high avidity binding to vascular selectins. *J. Immunol.* **160,** 5122–5129
39. Skrincosky, D., Kain, R., El-Battari, A., Exner, M., Kerjaschki, D., and Fukuda, M. (1997) Altered Golgi localization of core 2β-1,6-*N*-acetylglucosaminyltransferase leads to decreased synthesis of branched *O*-glycans. *J. Biol. Chem.* **272,** 22695–22702
40. Whitehouse, C., Burchell, J., Gschmeissner, S., Brockhausen, I., Lloyd, K. O., and Taylor-Papadimitriou, J. (1997) A transfected sialyltransferase that is elevated in breast cancer and localizes to the medial/trans-Golgi apparatus inhibits the development of core-2-based *O*-glycans. *J. Cell Biol.* **137,** 1229–1241
41. Priatel, J. J., Chui, D., Hiraoka, N., Simmons, C. J., Richardson, K. B., Page,

D. M., Fukuda, M., Varki, N. M., and Marth, J. D. (2000) The ST3Gal-I sialyltransferase controls CD8+ T lymphocyte homeostasis by modulating *O*-glycan biosynthesis. *Immunity* **12,** 273–283

42. Ellies, L. G., Tsuboi, S., Petryniak, B., Lowe, J. B., Fukuda, M., and Marth, J. D. (1998) Core 2 oligosaccharide biosynthesis distinguishes between selectin ligands essential for leukocyte homing and inflammation. *Immunity* **9,** 881–890
43. Snapp, K. R., Heitzig, C. E., Ellies, L. G., Marth, J. D., and Kansas, G. S. (2001) Differential requirements for the *O*-linked branching enzyme core 2β1–6-*N*-glucosaminyltransferase in biosynthesis of ligands for E-selectin and P-selectin. *Blood* **97,** 3806–3811
44. Piller, F., Piller, V., Fox, R. I., and Fukuda, M. (1988) Human T-lymphocyte activation is associated with changes in *O*-glycan biosynthesis. *J. Biol. Chem.* **263,** 15146–15150
45. Vachino, G., Chang, X. J., Veldman, G. M., Kumar, R., Sako, D., Fouser, L. A., Berndt, M. C., and Cumming, D. A. (1995) P-selectin glycoprotein ligand-1 is the major counter-receptor for P-selectin on stimulated T cells and is widely distributed in non-functional form on many lymphocytic cells. *J. Biol. Chem.* **270,** 21966–21974
46. Carlow, D. A., Gossens, K., Naus, S., Veerman, K. M., Seo, W., and Ziltener, H. J. (2009) PSGL-1 function in immunity and steady state homeostasis. *Immunol. Rev.* **230,** 75–96
47. Hirata, T., Furukawa, Y., Yang, B. G., Hieshima, K., Fukuda, M., Kannagi, R., Yoshie, O., and Miyasaka, M. (2004) Human P-selectin glycoprotein ligand-1 (PSGL-1) interacts with the skin-associated chemokine CCL27 via sulfated tyrosines at the PSGL-1 amino terminus. *J. Biol. Chem.* **279,** 51775–51782
48. León, B., and Ardavín, C. (2008) Monocyte migration to inflamed skin and lymph nodes is differentially controlled by L-selectin and PSGL-1. *Blood* **111,** 3126–3130
49. Orr, S. L., Le, D., Long, J. M., Sobieszczuk, P., Ma, B., Tian, H., Fang, X., Paulson, J. C., Marth, J. D., and Varki, N. (2013) A phenotype survey of 36 mutant mouse strains with gene-targeted defects in glycosyltransferases or glycan-binding proteins. *Glycobiology* **23,** 363–380